Advances in Medical Sciences 63 (2018) 127–133

Contents lists available at ScienceDirect

Advances in Medical Sciences

journal homepage: www.elsevier.com/locate/advms

Original research article

Ultrastructural characteristics of the respective forms of hepatic stellate cells in chronic hepatitis B as an example of high fibroblastic cell plasticity. The first assessment in children

Joanna Maria Lotowska[a,*], Maria Elzbieta Sobaniec-Lotowska[a], Dariusz Marek Lebensztejn[b]

[a] Department of Medical Pathomorphology, Medical University of Bialystok, 15-269 Bialystok, Waszyngtona Str. 13, Poland
[b] Department of Pediatrics, Gastroenterology and Allergology, Medical University of Bialystok, 15-274 Waszyngtona Str. 17, Poland

ARTICLE INFO

Article history:
Received 7 July 2017
Accepted 26 September 2017
Available online 6 November 2017

Keywords:
Quiescent HSCs (Q-HSCs)
Transitional HSCs (Ti-HSCs and Tp-HSCs)
Myofibroblastic HSCs (Mf-HSCs)
Liver fibrogenesis in children
Ultrastructure

ABSTRACT

Purpose: Activation of hepatic stellate cells (HSCs), mainly responsible for extracellular matrix synthesis, is assumed to be central event in the process of liver fibrogenesis. The major objective of the research was to analyze the ultrastructural profile of activated HSCs in children with chronic hepatitis B (chB), with respect to fibrosis intensity.

Materials/methods: Ultrastructural investigations of HSCs were conducted on liver bioptates from 70 children with clinicopathologically diagnosed chB before antiviral treatment. Biopsy material, fixed in paraformaldehyde and glutaraldehyde solution, was routinely processed for electron-microscopic analysis.

Results: In children with intensive liver fibrosis (S-2 and S-3), the ultrastructural picture showed almost total replacement of quiescent HSCs (Q-HSCs) by activated, i.e. transitional HSCs (T-HSCs). Among T-HSCs, two types of cells were distinguished: cells exhibiting initiation of HSC activation (Ti-HSCs), never before described in chB, that were frequently accompanied by activated Kupffer cells, and cells with features of perpetuation of activation (Tp-HSCs). Tp-HSCs were elongated and characterized by substantial loss of cytoplasmic lipid material; they contained an increased number of cytoskeletal components, extremely dilated channels of granular endoplasmic reticulum and activated Golgi apparatus, which indicated their marked involvement in intensive synthesis of extracellular matrix proteins. Many collagen fibers were found to adhere directly to Tp-HSCs.

Conclusions: The current study showed T-HSCs to be an important link between Q-HSCs and myofibroblastic HSCs (Mf-HSCs). Transformation of HSCs into new morphological variations (Ti-HSCs; Tp-HSCs and Mf-HSCs), observed along with growing fibrosis, indicates their high plasticity and a key role in fibrogenesis in pediatric chB.

1. Introduction

Hepatic stellate cells (HSCs), due to their morphology, biology and numerous functions within the organ, have long been defined in literature as a most fascinating and at the same time poorly known and enigmatic human cells [1]. The existence of numerous synonyms for this cell population, e.g. fat storing cells, Ito cells, perisinusoidal stellate cells, liver interstitial cells, liver specific pericytes or vitamin A storing cells seems to reflect the case [1–4]. It is assumed that HSCs belong to the population of nonparenchymal hepatic cells (NPCs), which apart from stellate cells accounting for approximately 20% of NPCs, also includes endothelial cells (c. 40%), Kupffer cells/macrophages (KCs/MPs) (c. 20%) and a heterogeneous subpopulation of intrahepatic lymphocytes (c. 20%) [4].

HSCs are easy to identify using transmission electron microscopy (TEM) or immunohistochemical (IHC) stainings, especially for smooth muscle actin (alpha-SMA) and desmin [1–3,5,6,7], but not with routine histological staining. Ultrastructural investigations allowed researchers to distinguish three main morphological forms of HSCs, quiescent HSCs (Q-HSCs), transitional HSCs (T-HSCs) and myofibroblastic HSCs (Mf-HSCs) [1,3,8–11].

It is assumed that HSCs which undergo transformation to metabolically active T-HSCs and myofibroblast-type cells are

* Corresponding author at: Department of Medical Pathomorphology, Medical University of Bialystok, Waszyngtona Str. 13, 15-269 Bialystok, Poland. Tel.: +4885 748 5945; fax: +4885 748 5990.
E-mail address: joannalotowska@gmail.com (J.M. Lotowska).

https://doi.org/10.1016/j.advms.2017.09.002
1896-1126/

mainly responsible for the synthesis of protein components of the extracellular matrix (ECM) and play a key role in the initiation and progression of liver fibrosis [5,6,10,12–15]. They are also a potential target for the treatment of liver fibrosis [12,14,15,16–19].

Up to now literature data on the sequence of morphological events observed at the ultrastructural level in the pathogenesis of liver fibrosis have been limited to adult patients and experimental studies. Similar reports on pediatric patients are lacking. Taking that into consideration, the aim of the current study was to characterize the respective forms of hepatic stellate cells in children with chronic hepatitis B (chB), in relation to the advancement of liver fibrosis, based on abundant retrospective biopsy material.

The study is a continuation of our many years' morphological and clinical research, including IHC and submicroscopic investigations, into the process of fibrogenesis and development of liver fibrosis in children with chB and other nonviral chronic diseases affecting this organ [20–25].

2. Material and methods

2.1. Study patients' profile

The retrospective morphological analysis was based on liver oligobiopsy specimens obtained blind from 70 children with chB (46 boys and 24 girls), aged 3–17 years (mean 11), who were qualified for alpha interferon or lamivudine treatment, but still prior to the initiation of scheduled antiviral therapy in the Department of Pediatrics, Gastroenterology and Allergology, Medical University of Bialystok. The patients had a documented HBV infection of >6 months' duration, with HBsAg and HBeAg-positive sera. Patients with HCV, with other liver disorders and with cirrhosis were excluded from the study.

In all study cases, the ultrastructural analysis of liver biopsies was preceded by semiquantitative numerical histologic assessment of the extent of liver fibrosis (staging – S) (using scoring system according to Batts and Ludwig – 26) as well as IHC staining for alpha SMA. The IHC and statistical results relative to the above patients were described in our earlier report [5]. All morphological investigations of the oligobiopsy material obtained from children with chB, together with TEM assessment, were performed in the Department of Medical Pathomorphology, Medical University of Bialystok.

The study was approved by the Bioethics Committee, Medical University of Bialystok.

2.2. Ultrastructural analysis

For ultrastructural investigations, small fresh liver blocks (1 mm^3 volume) were fixed in a solution containing 2% paraformaldehyde and 2.5% glutaraldehyde in 0.1 mol/L cacodylate buffer, pH 7.4. The specimens were postfixed in 2% osmium tetroxide (OsO_4) in 0.1 mol/L cacodylate buffer, pH 7.4, for 1 h. Then, the material was routinely processed for TEM analysis, i.e. dehydrated through a graded series of ethanols and propylene oxide, embedded in Epon 812 and sectioned on a Reichert ultramicrotome to obtain semithin sections (0.5–1 μm thick). These semithin sections were stained with 1% methylene blue in 1% sodium borate and examined under a light microscope. Ultrathin sections were double stained with uranyl acetate and lead citrate, and examined using an Opton 900 transmission electron microscope (Zeiss, Oberkochen, Germany). This processing procedure had been used in our earlier ultrastructural investigations of the liver in children [20–22].

HSCs were determined by a microscopist who was blinded to the clinical information.

3. Results

3.1. Baseline features

The semiquantitative numerical scoring system evaluating staging, i.e. the extent of liver fibrosis, according to Batts and Ludwig [26], preceding TEM analysis, allowed us to distinguish the following four study groups (from S-0 to S-3): group I (S-0) – consisting of 5 patients (2 boys; 3 girls); group II (S-1) – 27 patients (18 boys; 9 girls); group III (S-2) – 31 patients (21 boys; 10 girls) and group IV (S-3) – 7 patients (5 boys; 2 girls).

3.2. Group I (S-0)

EM analysis of the liver of children with chB in group I (S-0) allowed easy identification of dispersed Q-HSCs in biopsy specimens. They were observed in the perisinusoidal spaces of Disse, between sinusoidal endothelial cells and vascular pole of hepatocytes. They frequently intruded into the space in between adjacent hepatocytes. The presence of numerous lipid vacuoles exerting a pressure on cell organelles and constituting up to 80% of the cytoplasm volume was a characteristic feature of Q-HSCs (Fig. 1A,B). Among poorly developed cell organelles, narrow

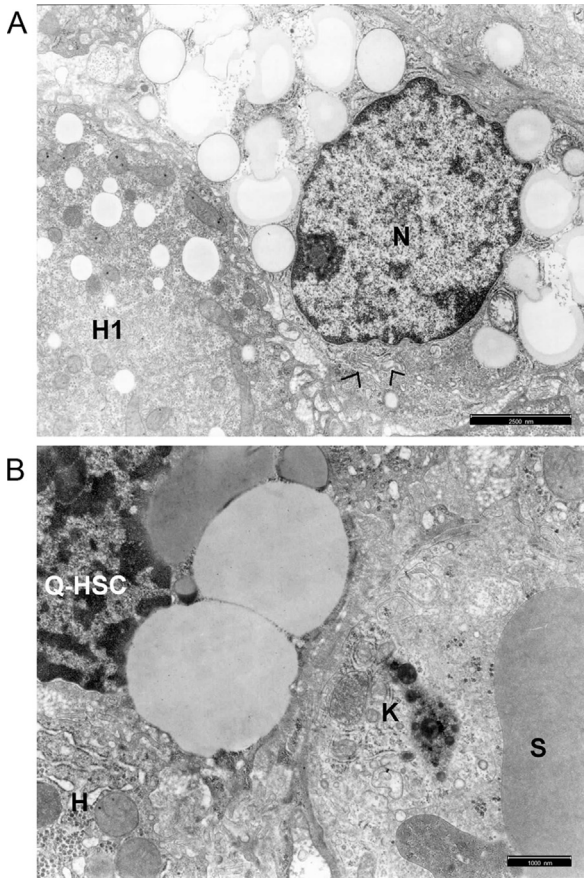

Fig. 1. 1A, 1B: The ultrastructure of quiescent HSCs (Q-HSCs) in biopsy material obtained from children with chB; group I (S-0).
A) The view of Q-HSC – located in the perisinusoidal space of Disse – filled up with lipid droplets; poorly developed cell organelles; visible Golgi apparatus in the perinuclear location (>); cell nucleus (N) contains abundance of euchromatin and heterochromatin mainly accumulating underneath the nuclear envelope and nucleolar body. The vascular pole of hepatocyte (H1) sends numerous microvilli towards Q-HSC (scale bar 2,5 μm, original magnification 4400×).
B) Fragment of Q-HSC containing large lipid droplets with an activated Kupffer cell (K) closely adhering to this cell. H – hepatocyte; S – sinusoidal lumen (scale bar 1 μm, original magnification 7000×).

granular endoplasmic reticulum (ger) channels and Golgi apparatus in the perinuclear region were most easy to identify (Fig. 1A). Q-HSCs had very fine dendritic cytoplasmic processes penetrating inside the surrounding extracellular matrix, where they "got lost" easily. Sometimes activated Kupffer cells/macrophages (KCs/MFs) were found closely adhering to them (Fig. 1B). Most of the observed images showed well preserved endothelial lining of sinusoidal capillaries, beneath which Q-HSCs were found.

3.3. Group II (S-1)

Apart from Q-HSCs, also HSCs showing features of variously pronounced activation, i.e. T-HSCs, were found in liver bioptates from S-1 patients.

Within the population of T-HSCs two subtypes of transitional cells can be distinguished. Type 1, observed more frequently in this group of children, i.e. cells exhibiting features of initiation of HSC activation (Ti-HSCs) (Fig. 2A–C), and type 2 (relatively seldom), i.e. cells in the phase of perpetuation of HSC activation (Tp-HSCs), whose ultrastructure will be presented with the study group III and IV.

The Ti-HSCs as compared to Q-HSCs were more elongated in shape and began to lose lipid material. Their cytoplasm often showed well developed, dilated ger channels filled up with delicate flocculent material and segmentally deprived of ribosomes (Fig. 2A,B). Sometimes the cytoplasm exhibited an activated zone of Golgi apparatus (Fig. 2B). The cell nucleus usually showed an abundance of focally clumping heterochromatin, as well as a nucleolus or a nucleolar body (Fig. 2A). Beneath the cell membrane of Ti-HSC, the cytoskeleton components were observed in the form of linearly arranged bundles of microfilaments (c. 5 nm in diameter) (Fig. 2C). Relatively frequently the perisinusoidal Ti-HSCs were surrounded by immature collagen fibers and the flocculent, condensed extracellular matrix (Fig. 2A), which can be referred to as a morphological precursor of collagen fibers.

Activated KCs/MFs quite frequently adhered directly or were adjacent to Ti-HSCs (Fig. 2B,C). They were enlarged and contained numerous primary and secondary phagosomes, varying in size and filled up with the phagocytized extracellular content (Fig. 2C). In comparison with group I, liver sinusoidal endothelial cells were swollen in some patients and showed features of defenestration, i.e. contained a smaller number of oval fenestrations that characteristic of normal sinusoidal endothelial cells.

3.4. Group III and IV (S-2 and S-3)

The ultrastructural pictures of the population of HSCs, both in group III and IV (S-2 and S-3), were very similar with respect to quality and quantity. These cells showed either perisinusoidal location (Figs. 3 A,B; 4 B) or were observed outside the space of Disse, in the spaces between hepatocytes (Figs. 3 C; 4 A) and within the foci of fibrosis (Fig. 4C–F).

Importantly, Q-HSCs were found relatively seldom in patients with intensive liver fibrosis. Instead, two types of activated HSCs were observed. In children with S-2, Ti-HSCs and Tp-HSCs were found in a similar proportion, whereas in patients with S-3 Tp-HSCs were predominant. Also myofibroblastic type HSCs, i.e. Mf-HSCs were present.

HSCs showing features of perpetuation of activation, i.e. Tp-HSCs, encountered mainly in the vicinity or within the sites of marked fibrosis, differed from Ti-HSCs in a more elongated cell body and its processes and by far greater loss of lipid material (Figs. 3 A,C; 4 A,C). The volume of the lipid material within Tp-HSCs constituted less or sometimes even much less than 20% of the cytoplasm volume. The cytoplasm of such cells could even contain a single drop or a very tiny lipid droplet, with the volume much

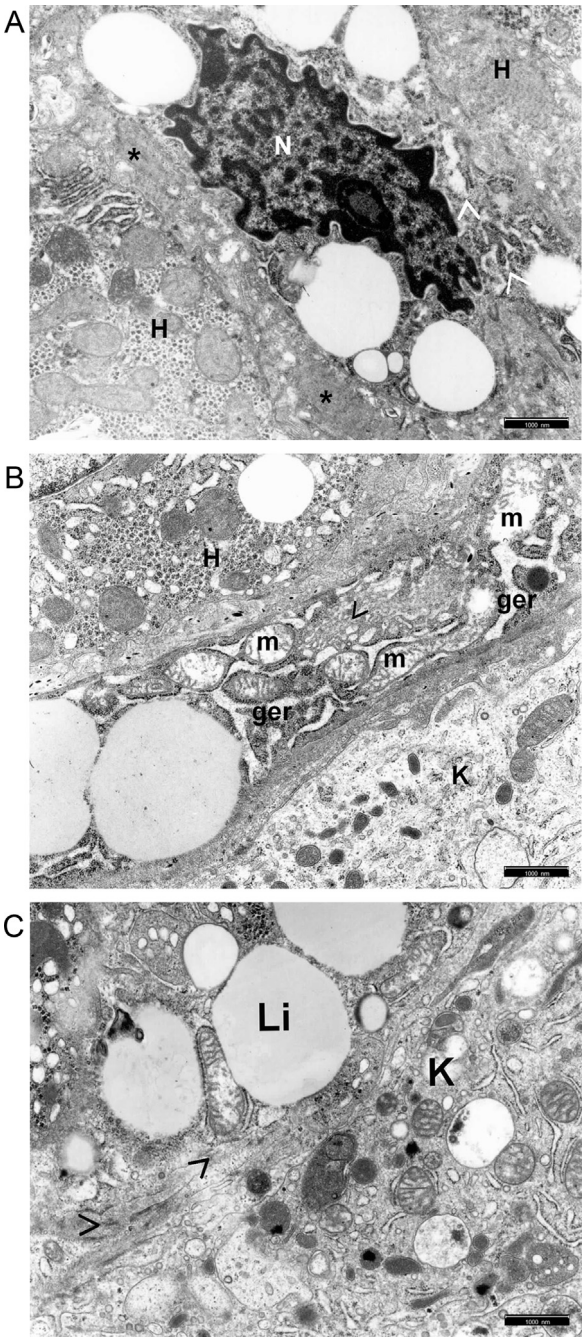

Fig. 2. A–C: Electron micrographs of activated forms of HSCs in biopsy material obtained from children with chB; group II (S-1).
A) The picture of HSC showing features of slight activation (Q-HSC transforming to Ti-HSC), located in the space between hepatocytes (H) which contains a centrally situated nucleus (N) with a nucleolar body, lipid droplets on the periphery and well developed slightly dilated ger components (>); the cell is enclosed by thickened extracellular matrix (*) (scale bar 1 μm, original magnification 7000×).
B) In the space of Disse – fragment of elongated transitional HSC-type cell (Ti-HSC being transformed to Tp-HSC), to which Kupffer cell/macrophage (K) adheres. The Ti-HSC lost a considerable part of lipid material; it contains markedly dilated channels of the granular endoplasmic reticulum (ger) and well-developed Golgi apparatus (>); some mitochondria (m) exhibit features of focal swelling. H – hepatocyte (scale bar 1 μm, original magnification 7000×).
C) Fragment of transitional HSC showing features of activation initiation (Ti-HSC), closely adhering to an apparently activated Kupffer cell/macrophage (K), which contains numerous cytoplasmic structures of primary and secondary phagosomal nature. Focally, cytoskeleton components (>) are present beneath the cell membrane of Ti-HSC (>); Li – lipid material of the cell (scale bar 1 μm, original magnification 12 000×).

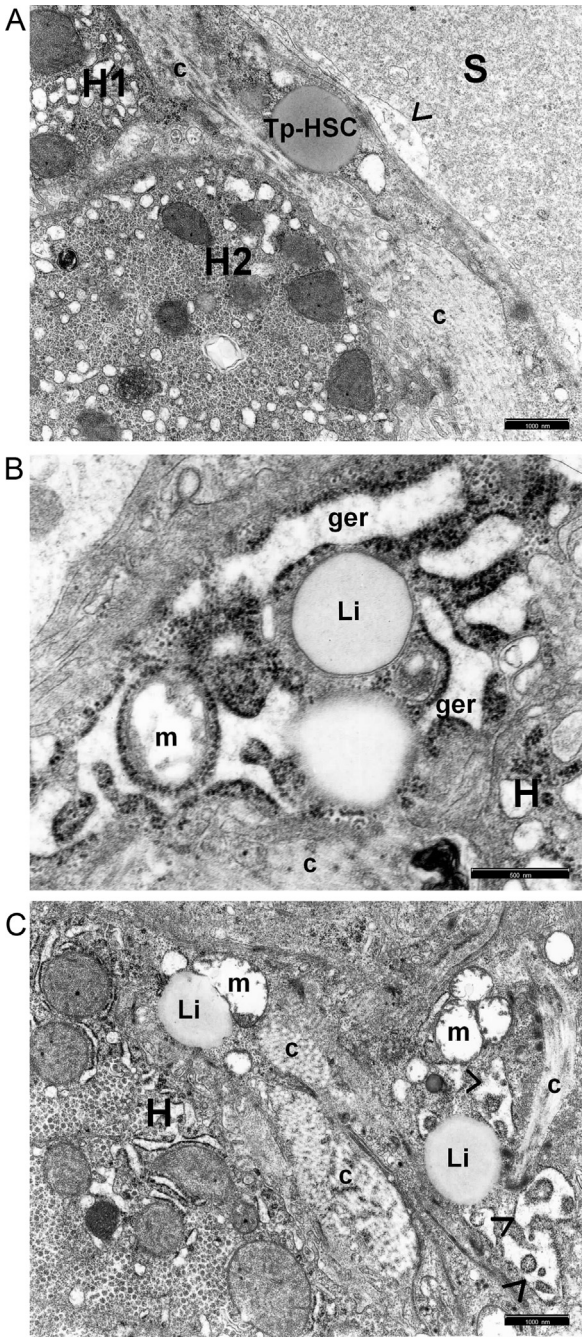

Fig. 3. A–C: The ultrastructure of activated forms of HSCs in biopsy material obtained from children with chB; group III (S-2).
A) In the dilated space of Disse there is a fusiform, thinned, markedly elongated Tp-HSC-type cell, reaching two adjacent hepatocytes (H1, H2) and abundance of collagen fibers (c). The vascular poles of hepatocytes directed towards the perisinusoidal space – smoothed; endothelial lining (>) swollen in places; S – sinusoidal vascular lumen (scale bar 1 μm, original magnification 7000×).
B) Large magnification of a fragment of a perisinusoidal Tp-HSC very well demonstrating cisternally dilated ger channels, segmentally deprived of ribosomes and containing fine flocculent material; visible swollen mitochondrion (m), single lipid droplets (Li) and the cytoplasm area with abundance of free ribosomes (*). Below the cell, collagen (c) and fine biliary deposit. The vascular pole of the hepatocyte (H) – smoothed (scale bar 0,5 μm, original magnification 20 000×).
C) The picture of two cells of Tp-HSC type pushed in the space between hepatocytes and containing a small amount of lipid material (Li), degenerating mitochondria (m) and cisternally dilated ger channels (>). Above, Tp-HSC, prominently thinned and elongated, with long and fine cytoplasmic processes. In close vicinity of the Tp-HSCs thick bundles of collagen fibers (c) are seen; H – fragment of hepatocyte (scale bar 1 μm, original magnification 7000–).

smaller than 10% of the cytoplasm volume (Fig. 4A). The ger channels were expanded and markedly dilated, often more than in Ti-HSCs, forming cistern-like structures filled up with delicate flocculent material (Figs. 3 B, C; 4 A). Greater degranulation of ger channels and areas of the cytoplasm filled with free ribosomes were noted (Figs. 3 B; 4 B). An expanded zone of Golgi apparatus was found in the perinuclear region (Fig. 4A). Mitochondria showed features of variously pronounced swelling and/or degenerative lesions, mainly such as considerable loss of cristae (Fig. 3B, C) and myelinic structures being formed within their matrix. Numerous bundles of microfilaments running parallel to one another were found to accumulate beneath the cell membrane (Fig. 4B). The cytoplasmic processes of Tp-HSCs were markedly elongated, thinned and sometimes reached neighboring hepatocytes (Fig. 3A).

However, the myofibroblastic type HSCs were frequently observed within the fibrotic foci (Fig. 4D–F). Mf-HSCs were elongated, sometimes even more than Tp-HSCs. Their cytoplasm contained well-developed, abundant and frequently markedly dilated ger, expanded Golgi apparatus and trace amount of lipid material (Fig. 4D–F). Beneath the membrane, the cytoplasm showed greater agglomerations of the linearly arranged bundles of microfilaments as compared to Tp-HSCs, with the presence of the so called dense areas (Fig. 4D,E). Typical fibroblasts were sometimes present in their vicinity.

It should be emphasized that patients with S-2 and S-3 demonstrated an abundance of bundles of mature collagen fibers closely adhering to Tp-HSC and Mf-HSC bodies and/or their cytoplasmic processes (Figs. 3 A,C; 4 A–D,F). Many times these cells, especially in S-3, appeared “embedded” in massive collagen deposits forming fine “scarring” of the parenchyma (Fig. 4C,F). Some Mf-HSCs underwent substantial shrinkage and distinct degenerative lesions, including disintegration. (Fig. 4F).

The above changes in the population of HSCs were accompanied by marked damage to the vascular pole of hepatocytes and sinusoidal endothelial lining. The vascular pole of hepatocytes directed to the dilated space of Disse, towards the surface of T-HSCs, was usually smoothed and deprived of microvilli (Fig. 3A,B). However, endothelial cells of the sinusoidal vessels frequently showed features of substantial swelling and defenestration; sometimes distinct degenerative lesions, including disintegration, were noted (Figs. 3 A; 4 B).

4. Discussion

The current study is the first electron-microscopic analysis of HSCs in ample biopsy material obtained from pediatric patients with chB. Previously, our IHC research in the same group of children with chB showed a close positive correlation of HSC count with liver fibrosis intensity, which confirms their crucial role in the development and progression of this pathology [5]. Interestingly, the highest mean number of immunoreactive HSCs/100 hepatocytes was found in the intermediate zone of the hepatic lobule, which suggests that this area of the lobule is most metabolically active in the process of liver fibrogenesis [5].

In children with chB accompanied by intensive liver fibrosis (S-2 and S-3), the ultrastructural picture showed almost total replacement of Q-HSCs by activated HSCs, i.e. HSCs referred to as the transitional or myofibroblastic type. Apart from perisinusoidal location, T-HSCs and Mf-HSCs were also found in the vicinity or/and within the fibrotic foci being formed or already developed, the so called “collagen scars” of the liver. Interestingly, the activation of HSCs was accompanied by changes in other NPCs, i.e. KCs/MFs and liver sinusoidal endothelial cells, which will be the subject of our future in-depth submicroscopic analysis.

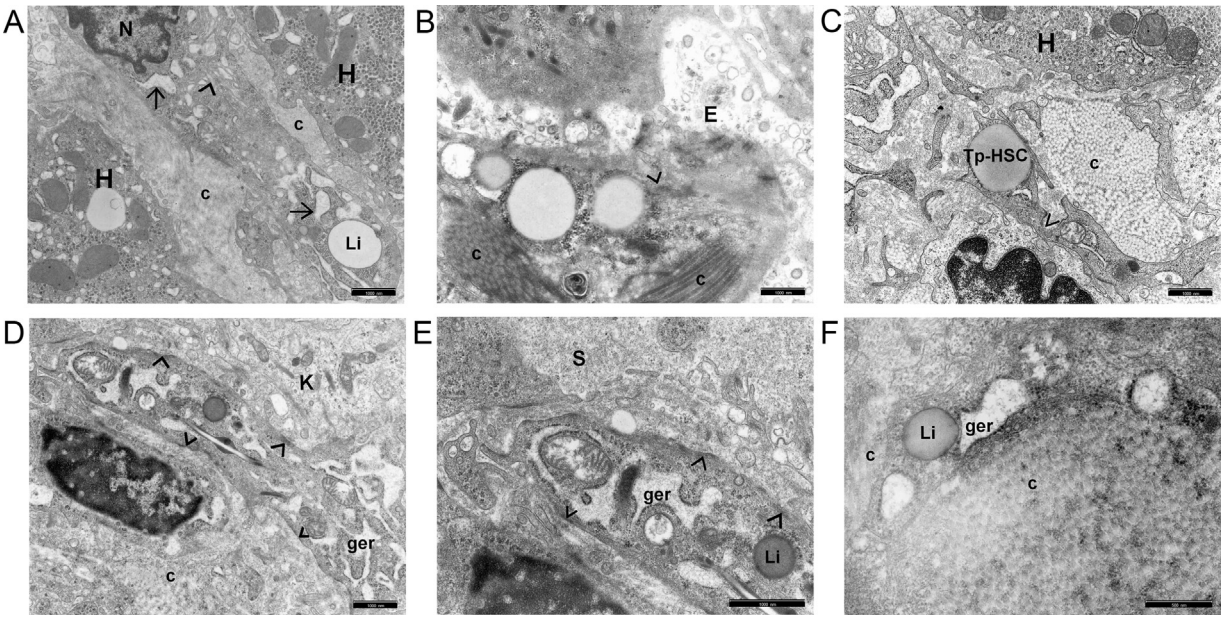

Fig. 4. A–F: Electron micrographs of activated forms of HSCs in biopsy material obtained from children with chB; group IV(S-3).
A) The space between hepatocytes shows a centrally located Tp-HSC. Cisternally dilated ger channels (- >), segmentally deprived of ribosomes; well-developed Golgi apparatus (>), a single lipid droplet (Li) and a fragment of cell nucleus (N). The cell is surrounded by the abundance of collagen connective tissue in the form of thick bundles of fibers that exert pressure on the cell (c) (scale bar 1 μm, original magnification 7000×).
B) Fragment of a Tp-HSC type cell lies underneath markedly swollen endothelial lining (E) of a sinusoidal vessel. It contains lipid droplets, large number of free ribosomes and bundles of microfilaments accumulating beneath the membrane (>); the cell is surrounded by a thick bundle of collagen fibers (c); extracellular tiny biliary deposit is visible; basement membrane of the sinusoidal vessel is focally thickened (scale bar 1 μm, original magnification 12 000×).
C) The central part of the electronogram exhibits a distinctly elongated Tp-HSC with numerous cytoplasmic processes. This cell contains a single peripherally located lipid droplets and slightly dilated ger channels. In the vicinity, transverse sections through the abundance of collagen bundles (c) forming a fine collagen "scar", intruding focally into the cell (>); above a hepatocyte fragment (H). A bioptate obtained from the borderline plate of the liver lobule (scale bar 1 μm, original magnification 7000×).
D) E) A markedly elongated HSC, with cytoplasmic processes, myofibroblastic in nature (Mf-HSC) and a mononuclear inflammatory cell seen on the margin of a fibrotic focus (c). Within the Mf-HSC in the foreground – well developed ger components, cisternally dilated and segmentally deprived of ribosomes; a single lipid droplet; accumulation of submembranous cytoskeleton components (>) K – fragment of Kupffer cell/macrophage; S – sinusoidal vascular lumen (**D**: scale bar 1 μm, original magnification 7000×; **E:** scale bar 1 μm, original magnification 12 000×).
F) Large magnification of a fine collagen scar of the liver containing a fragment of distinctly constricted, elongated and degenerated Mf-HSC. It is "embedded" in collagen (c). The electron-dark cytoplasm shows cisternally dilated ger channels, filled up with fine fibrillary content, areas with numerous free ribosomes and a single lipid droplet (Li); the cell merges in places with the surrounding collagen fibers (scale bar 1 μm, original magnification 20 000×).

We distinguished 2 types of cells among T-HSCs, namely cells exhibiting initiation of activation (Ti-HSCs), which began to appear earlier, i.e. in the first phase of fibrosis (S-1) and cells showing features of perpetuation of activation (Tp-HSCs). This is consistent with our preliminary observations referring to the morphology of these cells [24]. Worthy of mention is that we were the first in hepatological literature to separate Ti-HSCs out of the T-HSC pool in patients with chB based on the current ultrastructural investigations.

In comparison with Q-HSCs, Ti-HSCs were more elongated, had dilated ger channels and began to lose cell-typical lipid material. They were frequently enclosed by the condensed extracellular matrix, being a likely morphological precursor of collagen fibers. However, Tp-HSCs had elongated body and processes, by far more than Ti-HSCs, and showed greater loss of cytoplasmic lipid material; bundles of contractile microfilaments were seen beneath the cell membrane. Their ger channels were well-developed and more dilated, with a great loss of ribosomes and markedly activated zone of Golgi apparatus, which indicated an essential role of these cells in the intensive synthesis and transport of ECM. Interestingly, in the vicinity of T-HSCs, especially Ti-HSCs, activated KCs/MPs were found.

On the other hand, Mf-HSCs, also called "wound healing" myofibroblasts, found in fibrotic foci, were even more elongated than Tp-HSCs; they contained well-developed and markedly dilated ger (features typical of fibroblasts) and greater submembranous accumulation of microfilament bundles. They were characterized by almost total loss of lipid material.

Abundant quantities of thick bundles of mostly mature collagen fibers frequently adhered directly to Tp-HSCs and Mf-HSCs. It is assumed that these cells, irrespective of the cause of fibrosis, generate around themselves new collagen fibers, thus leading to the process of fibrosis [2,8,10–12,14,15].

The T-HS type cells, due to their interesting morphological picture and the key role in the process of fibrogenesis and the progression of fibrosis, have received special treatment in hepatology [1,9,12,14,15]. Fascinated by this mysterious cell population, Friedman [1] in a broad and in-depth manuscript on the biology of hepatic stellate cells obtained from tissue culture and their role in experimental liver fibrogenesis defined them as "multifunctional and enigmatic cells".

The ultrastructure of T-HSCs in the current analysis resembled considerably the one described in the studies on liver fibrogenesis in adult patients with chronic liver disorders, and in experimental models of liver fibrosis, including common bile duct ligation or long-term use of hepatoxins, especially carbon tetrachloride and thioacetamide [1,3,8,11,17,27]. It is assumed that due to the loss of lipid material, i.e. retinoids, such as retinol palmitate (vitamin A) and triacylglycerol accumulated in the cytoplasmic lipid droplets, and due to the extended and dilated ger channels, T-HSCs are converted into the major, i.e. intermediate, link between Q-HSCs and Mf-HSCs [1,8,9,11,15,17,24].

Numerous experimental and morphological-clinical reports on liver fibrogenesis, limited however to adult patients, have emphasized a major role of HSCs in intercellular communication [6,10,12,13,28–30]. According to some researchers, the earliest changes observed in the process of HSC activation were due to paracrine stimulation by all types of cells adjacent to stellate cells, including KCs, sinusoidal endothelial cells, hepatocytes and blood platelets [2,4,15,18,31,32]. These observations are confirmed by our current results indicating that early submicroscopic abnormalities in the population of HSCs were accompanied by distinct changes in the population of adjacent KCs/MFs and endothelial cell lining of sinusoidal vessels. It is assumed that KCs by the release of cytokines activate proliferation of HSCs and retinoid release from them, which results in the intensified expression of genes responsible for ECM protein synthesis [1,2,10,31–33].

With regard to the role of hepatic sinusoidal endothelial cells in the process of liver fibrogenesis it is assumed that their damage triggers production of cell fibronectin which activates HSCs [30]. Endothelial cells are also likely to be responsible for the conversion of TGF-B from the latent form to the active type, i.e. profibrogenic form [29]. Worthy of mention is also the role of the angiogenic marker – vascular endothelial growth factor (VEGF) in fibrotic pathogenesis, which promotes the activation of HSCs in chronic liver diseases [7,34]. Latest histopathologic and IHC analyses demonstrate the relations between VEGF expression and the activated HSCs represented by the expression of alpha-SMA in chronic hepatitis C biopsies and suggest that both factors can be used as a predictor for the progression of fibrosis [7].

In summary, the ultrastructural picture of the extremely interesting heterogenous and multifunctional HSCs shows that submicroscopic changes in these cells in the course of liver fibrogenesis are relatively discrete in the initial phase of cell activation, gradually enhanced along with fibrosis intensity and fully developed in the phase of perpetuation of activation. They eventually acquire features of myofibroblastic stellate cells.

The results of the current research should be treated as a preliminary study that have to be continued on a well-defined group of patients with chB and compared with ultrastructural observations of activated HSCs made by other research centres.

5. Conclusions

As shown by the current study, T-HSCs constitute an important link, i.e. intermediate cell link, between Q-HSCs and Mf-HSCs in hepatic fibrogenesis in children with chB. Transformation of Q-HSCs into their new morphological variations (Ti-HSCs; Tp-HSCs and Mf-HSCs) and their relations with the adjacent perisinusoidal cells observed along with a growing extent of fibrosis indicate high fibroblastic plasticity of this NPC population and their key role in the initiation and progression of collagen fibroplasia. In our opinion, the submicroscopic assessment of HSCs, constituting the main type of fibrocompetent cells in the liver, may throw more light onto the role of these cells in the process of fibrogenesis and can be a valuable prognostic factor in fibrosis progression. The results of current ultrastructural investigations have allowed a better understanding of the dynamics of fibrosis and may be an interesting comparative material for similar findings on the biology of heterogenous HSCs in children with chB, providing new insights into potential treatments for hepatic fibrosis.

Conflict of interests

The authors declare no conflict of interests.

Financial disclosure

The authors have no funding to disclose.

References

[1] Friedman SL. Hepatic stellate cells: protean, multifunctional, and enigmatic cells of the liver. Physiol Rev 2008;88(1):125–78.
[2] Senoo H, Yoshikawa K, Morii M, Miura M, Imai K, Mezaki Y. Hepatic stellate cell (vitamin A-storing cell) and its relative–past, present and future. Cell Biol Int 2010;34(12):1247–72.
[3] Bartók I, Virágh S, Hegedüs C, Bartók K. Ultrastructure of the Ito cells in liver disease associated with fibrosis. Acta Morphol Hung 1989;37(3-4):219–34.
[4] Mehal WZ, Azzaroli F, Crispe IN. Immunology of the healthy liver: old questions and new insights. Gastroenterology 2001;120(1):250–60.
[5] Lotowska JM, Lebensztejn DM. Immunoreactive hepatic stellate cells in biopsy material in children with hepatitis B: the first report in children. Pol J Pathol 2015;66(3):224–30.
[6] Kagan P, Sultan M, Tachlytski I, Safran M, Ben-Ari Z. Both MAPK and STAT3 signal transduction pathways are necessary for IL-6-dependent hepatic stellate cells activation. PLoS One 201712(May (5))e0176173.
[7] Elzamly S, Agina HA, Elbalshy AE, Abuhashim M, Saad E, Abd Elmageed ZY. Integration of VEGF and α-SMA expression improves the prediction accuracy of fibrosis in chronic hepatitis C liver biopsy. Appl Immunohistochem Mol Morphol 2016(March) Epub ahead of print.
[8] Mansy SS, Elkhafif NA, Abelfatah AS, Yehia HA, Mostafa I. Hepatic stellate cells and fibrogenesis in hepatitis C virus infection: an ultrastructural insight. Ultrastruct Pathol 2010;34(2):62–7.
[9] Tsuchida T, Friedman SL. Mechanisms of hepatic stellate cell activation. Nat Rev Gastroenterol Hepatol 2017(May), doi:http://dx.doi.org/10.1038/nrgastro.2017.38 Epub ahead of print.
[10] Zhou WC, Zhang QB, Qiao L. Pathogenesis of liver cirrhosis. World J Gastroenterol 2014;20(23):7312–24.
[11] Nepomnyashchikh GI, Aidagulova SV, Nepomnyashchikh DL, Kapustina VI, Postnikova OA. Ultrastructural and immunohistochemical study of hepatic stellate cells over the course of infectious viral fibrosis and cirrhosis of the liver. Bull Exp Biol Med 2006;142(6):723–8.
[12] Zhang CY, Yuan WG, He P, Lei JH, Wang CX. Liver fibrosis and hepatic stellate cells: etiology, pathological hallmarks and therapeutic targets. World J Gastroenterol 2016;22(48):10512–22.
[13] Hong JS, Lee DH, Yook YW, Na D, Jang YJ, Kim JH, et al. MicroRNA signatures associated with thioacetamide-induced liver fibrosis in mice. Biosci Biotechnol Biochem 2017;4(April)1–8, doi:http://dx.doi.org/10.1080/09168451.2017.1308242 Epub ahead of print.
[14] Mehal WZ, Schuppan D: Antifibrotic therapies in the liver. Semin Liver Dis 2015;35(2):184–98.
[15] Higashi T, Friedman SL, Hoshida Y. Hepatic stellate cells as key target in liver fibrosis. Adv Drug Deliv Rev 2017(May), doi:http://dx.doi.org/10.1016/j.addr.2017.05.007 pii: S0169-409X(17)30063-7, Epub ahead of print.
[16] Guo Z, Li D, Peng H, Kang J, Jiang X, Xie X, et al. Specific hepatic stellate cell-penetrating peptide targeted delivery of a KLA peptide reduces collagen accumulation by inducing apoptosis. J Drug Target 2017;7(May)1–9, doi:http://dx.doi.org/10.1080/1061186X.2017.1322598 Epub ahead of print.
[17] El Taghdouini A, Najimi M, Sancho-Bru P, Sokal E, van Grunsven LA. In vitro reversion of activated primary human hepatic stellate cells. Fibrogenesis Tissue Repair 2015;8(August):14.
[18] Campana L. Iredale JP: regression of liver fibrosis. Semin Liver Dis 2017;37(1):1–10.
[19] Najar M, Fayyad-Kazan H, Faour WH, El Taghdouini A, Raicevic G, Najimi M, et al. Human hepatic stellate cells and inflammation: a regulated cytokine network balance. Cytokine 2017;90:130–4.
[20] Sobaniec-Lotowska ME, Lotowska JM, Lebensztejn DM. Ultrastructure of oval cells in children with chronic hepatitis B, with special emphasis on the stage of liver fibrosis: the first pediatric study. World J Gastroenterol 2007;13(21):2918–22.
[21] Sobaniec-Lotowska ME, Lebensztejn DM, Lotowska JM, Kanczuga-Koda L, Sulkowski S. Ultrastructure of liver progenitor/oval cells in children with nonalcoholic steatohepatitis. Adv Med Sci 2011;56(2):172–9.
[22] Lotowska JM, Sobaniec-Lotowska ME, Lebensztejn DM. The role of Kupffer cells in the morphogenesis of nonalcoholic steatohepatitis – ultrastructural findings. The first report in pediatric patients. Scand J Gastroenterol 2013;48(3):352–7.
[23] Lotowska JM, Sobaniec-Lotowska ME, Bockowska SB, Lebensztejn DM. Pediatric non-alcoholic steatohepatitis: the first report on the ultrastructure of hepatocyte mitochondria. World J Gastroenterol 2014;20(15):4335–40.
[24] Lotowska JM, Lebensztejn DM. Ultrastructure of activated stellate cells (HSCs) in liver fibrogenesis in the course of chronic hepatitis B. The first study in pediatric patients. Pol J Pathol 2016;67(Suppl. 1):61–2.
[25] Lotowska JM, Sobaniec-Lotowska ME, Daniluk U, Lebensztejn DM. Glassy droplet inclusions within the cytoplasm of Kupffer cells: a novel ultrastructural feature for the diagnosis of pediatric autoimmune hepatitis. Dig Liver Dis 2017(April), doi:http://dx.doi.org/10.1016/j.dld.2017.04.001 pii: S1590-8658(17)30809-5. Epub ahead of print.

[26] Batts KP, Ludwig J. Chronic hepatitis: an update on terminology and reporting. Am J Surg Pathol 1995;19(12):1409–17.
[27] Lotowska JM, Sobaniec-Lotowska ME, Lebensztejn DM, Daniluk U, Sobaniec P, Sendrowski K, et al. Ultrastructural characteristics of rat hepatic oval cells and their intercellular contacts in the model of biliary fibrosis. New insights into experimental liver fibrogenesis. Gastroenterol Res and Pract 2017 2721547.
[28] Gressner OA, Lahme B, Demirci I, Gressner AM, Weiskirchen R. Differential effects of TGF-beta on connective tissue growth factor (CTGF/CCN2) expression in hepatic stellate cells and hepatocytes. J Hepatol 2007;47 (5):699–710.
[29] Beljaars L, Daliri S, Dijkhuizen C, Poelstra K, Gosens R. WNT-5A regulates TGF-β-related activities in liver fibrosis. Am J Physiol Gastrointest Liver Physiol 2017;312(3):G219–27.
[30] Liu XY, Liu RX, Hou F, Cui LJ, Li CY, Chi C, et al. Fibronectin expression is critical for liver fibrogenesis in vivo and in vitro. Mol Med Rep 2016;14(4):3669–75.
[31] Bilzer M, Roggel F, Gerbes AL. Role of Kupffer cells in host defense and liver disease. Liver Int 2006;26(10):1175–86.
[32] Heymann F, Trautwein C, Tacke F. Monocytes and macrophages as cellular targets in liver fibrosis. Inflamm Allergy Drug Targets 2009;8(4):307–18.
[33] Ikejima K, Okumura K, Lang T, Honda H, Abe W, Yamashina S, et al. The role of leptin in progression of non-alcoholic fatty liver disease. Hepatol Res 2005;33 (2):151–4.
[34] Luo J, Liang Y, Kong F, Qiu J, Liu X, Chen A, et al. Vascular endothelial growth factor promotes the activation of hepatic stellate cells in chronic schistosomiasis. Immunol Cell Biol 2017(January), doi:http://dx.doi.org/10.1038/icb.2016.109 Epub ahead of print.